

Zinc Electrochemical Deposition from Ionic Liquids and Aqueous Solutions Onto indium tin oxide.

F. M. Rivas-Esquivel^{1,2}, G.M. Brisard², R. Ortega-Borges^{1,*}, G. Trejo¹, Y. Meas¹

¹Centro de Investigación y Desarrollo Tecnológico en Electroquímica (CIDETEQ), Parque Tecnológico Querétaro Sanfandila. C.P. 76703 Pedro Escobedo, Qro., México.

²Faculté de Sciences, Université de Sherbrooke, 2500, Boulevard de l'Université Sherbrooke, QC, Canada J1K 2R1

*E-mail: rortega@cideteq.mx

Received: 11 November 2016 / Accepted: 20 January 2017 / Published: 12 February 2017

Ionic Liquids (ILs) are classified as green solvents and in this context, ILs offer the possibility to improve the electrodeposition processes of several metals or alloys, without involve the use of hazardous chemicals. In this work, we study the electrodeposition process of metallic zinc from the protic ionic liquid 2-hydroxyethyl ammonium propionate (2-HEAP) and from acidic aqueous solutions on indium tin oxide (ITO) as substrate. Electrodeposits obtained from 2-HEAP by using different zinc salts as a source of metallic ions are compared with electrodeposits obtained from aqueous solutions. Results show the influence of zinc salt and of the reaction media (2-HEAP or aqueous solutions) on the electrochemical reduction process and on the morphological properties of the deposits.

Keywords: Zinc electrodeposition, ITO, protic ionic liquids, Zn coatings.

1. INTRODUCTION

The interest in the study of Zn electrodeposition is related to the applications of metallic zinc coatings in several industrial and technological fields [1]. For these reasons, Zn electrodeposition is one of the more important electrochemical processes for surface treatment because of its application in anticorrosion protection [2] and also as an electrode material in Zn batteries [3]. Zn electrodeposits are obtained from the direct electrochemical reduction of solutions containing Zn^{2+} . In this way, in addition to the very negative potential needed to carry out the reduction of Zn^{2+} to Zn, the main limitation of the Zn electrodeposition from acidic or basic solutions in aqueous media is associated to the simultaneous hydrogen evolution reaction (HER) [4] limiting the faradic efficiency of the electrochemical processes. The HER has also a direct effect on the nucleation and on the

electrocrystallization of zinc [5] because of high cathodic currents are required to the reduction processes that induces dendritic deposits and make it difficult to control the grain size. This effect adversely affects the physical and the structural properties of the zinc electrodeposits, e.g. poor adhesion, inhomogeneous deposits, etc.

Concerning the electrodeposition of metallic zinc, it is necessary to consider that when Zn^{2+} solutions are electrolyzed from aqueous media, two electrodeposition processes in competition can be carried out: either metallic zinc (Zn) or zinc oxide (ZnO) deposition. ZnO can be indirectly obtained by induced precipitation when Zn^{2+} aqueous solutions are electrolyzed and a raise in the interfacial pH is produced [6]. ZnO is a transparent n-type semiconductor with a bandgap of 3.3 eV [7] and shows conductive properties. ZnO thin layers are interesting for their potential optical, photovoltaic, photocatalytic [8] and optoelectronics applications [9]. The efficiency in the electrochemical indirect electrodeposition of ZnO from aqueous solutions is also affected by the simultaneous HER and the competition between the process of formation of zinc oxide and the formation of hydroxides or mixed salts.

Due to the disadvantages associated to Zn or ZnO electrodeposition from aqueous medium, there are permanent efforts to design new electrodeposition processes and to optimize the existing processes on a basis of more selective and inexpensive processes in order to obtain pure and homogeneous electrodeposits [10], with a minor production of toxic wastes and eliminating or reducing the simultaneous hydrogen evolution reaction and the formation of hydroxides or mixed salts. In this paper we explore an alternative way to electrodeposits Zn using ionic liquids at room temperature. Room-temperature ionic liquids (RTILs) are currently an alternative group of green solvents [11,12] promising a revolution in synthetic chemistry [13-15] because of a large number of compounds with anions and cations of very different chemical nature can be used [16]. RTILs have attracted much attention in recent years [17], their electrochemical applications have been highly explored [18-20] and many new applications beyond green chemistry [21, 22] continue to be found. RTILs can be classified as protic (PILs) or aprotic ILs (AILs) [14]. AILs have been studied to be employed in several fields, including electrodeposition [23]; contrariwise, for PILs applications are less studied; however, major efforts are carried out to develop PILs involving simple and lineal cations and anions to improve the electrodeposition of several metals, including zinc.

Most of know ILs have wide electrochemical windows, high thermal stability, good ionic conductivity [24] and null vapor pressure [25]. Combined with metallic salts dissolution possibility, ionic liquids can be good candidates [7], as compared with aqueous solutions, for a wide range of metals and alloys electroplating [26] (Cr or Cr(III) [27-28], Al of aluminates [29,30], etc.), with the possibility of being use as electrolyte without additives or complex solutions [31,32]. Also exists the possibility of obtaining nanostructured coatings [1, 18]. Furthermore the Zn and ZnO electrodeposits on different types of conductive substrates (metallic or based in transparent conductive oxides like ITO) show great interest for applications based on the functional properties of the deposits by example in corrosion protection, in depollution process based on the use of Zn as a zero valent metals, in photocatalysis, kesterite photovoltaics cells [33], etc. Therefore, in this work the electrodeposition processes of Zn and ZnO from 2-HEAP onto ITO (90% w/w In_2O_3 and 10% w/w SnO_2) is studied and

compared with results of electrodeposition from aqueous solution in order to determine the advantages of electrodeposition from PILs.

2. EXPERIMENTAL PROCEDURE

2.1. *Synthesis of the RTIL 2-hydroxyethyl ammonium propionate (2-HEAP)*

The RTIL was prepared by an acid-base neutralization reaction, between a Brönsted acid (propionic acid, 99.5% Sigma-Aldrich) and a Brönsted base (ethanolamine, 99% Sigma-Aldrich). Chemicals were slowly mixed, by continuous addition of the base to the acid drop to drop until an equimolar mixture was obtained. Mixture was carried out in a jacketed cell under argon atmosphere, and stirring was continued until a clear homogenous solution was obtained as reported earlier [34,35]. During all the synthesis the temperature was maintained at 0°C due to the highly exothermic reaction. After mixing was stopped, the reaction mixture was continuously stirred at room temperature for 24 hours. No pretreatment of chemicals was carried out before their use.

2.2. *Electrochemical experiments*

The electrochemical reduction of Zn(II) in 2-HEAP was studied by cyclic voltammetry and by chronoamperometric techniques. All electrochemical measurements were carried out by using an EG&G Princeton Applied Research Potentiostat/Galvanostat Model 273A controlled by a personal computer to apply the operation parameters of each electrochemical technique and for data acquisition. The electrochemical measurements were carried out at controlled temperature (25°C) in a standard three-compartment electrochemical cell. For the experiments in 2-HEAP a typical three electrodes electrochemical system was used: a 99.99% silver wire as a pseudo-reference electrode (pRE), a platinum mesh as counter electrode and an ITO plate ($A = 1\text{cm}^2$) as working electrode. Three zinc salts were used for the experiments (ZnCl_2 , $\text{Zn}(\text{C}_2\text{H}_3\text{O}_2)_2$ and $\text{Zn}(\text{C}_3\text{H}_5\text{O}_2)_2$), at a concentration of 0.05M in 2-HEAP. In aqueous solutions, the composition of the studied solution was 0.05 M ZnCl_2 and 0.4M H_3BO_3 . In this case, a three electrodes electrochemical system was also used but the reference electrode was a saturated calomel electrode (SCE).

2.3. *Physico-chemical characterization of Zn electrodeposits*

SEM and AFM microscopy techniques were used to characterize the morphology of the obtained Zn deposits; for them, the elemental composition was evaluated by EDS and the crystalline structure was determined by XRD; thickness was evaluated by AFM and profilometry measurements. SEM and EDS analysis were obtained from each sample analyzed using an SEM JSM – 5400 LV equipment with acceleration of 15keV and with a time of 2000 counts/seconds for each microanalysis obtained. For the AFM technique, a Dimension Icon Atomic Force Microscope with Scanasyt equipment in contact air and Scan Asyst air mode was used. The XRD spectra were recorded on a

XRD spectrometer Bruker D8 Advance Cu-source, theta-theta diffractometer with a Lynx-eye position sensitive detector. The measurements of profilometry were carried out using a Dektak® 6M benchtop stylus profilometer controlled by its software v8.30.005. In addition, adherence tests were carried out according to the ASTM D 3359–97: Standard Test Methods for Measuring Adhesion by Tape Test.

3. RESULTS AND DISCUSSION

Concerning the electrochemical behavior of 2-HEAP as a solvent, the electrochemical measurements show an electrochemical window of 1.76V, indicating the potential range of electrochemical stability of 2-HEAP. As shown in Fig 1, in the cathodic side, the limit is observed at -2V, associated to the electrochemical reduction reaction of the 2-hydroxyethylammonium cation; the anodic limit is imposed by the oxidation reaction of the propionate anion (-0.24V). The electrochemical stability was evaluated making a cut-off at $\pm 4\mu\text{A}/\text{cm}^2$ and taken the zone of electrochemical stability as the potential range comprised between a current density of $\pm 0.1\mu\text{A}/\text{cm}^2$ at 5 mV/s.

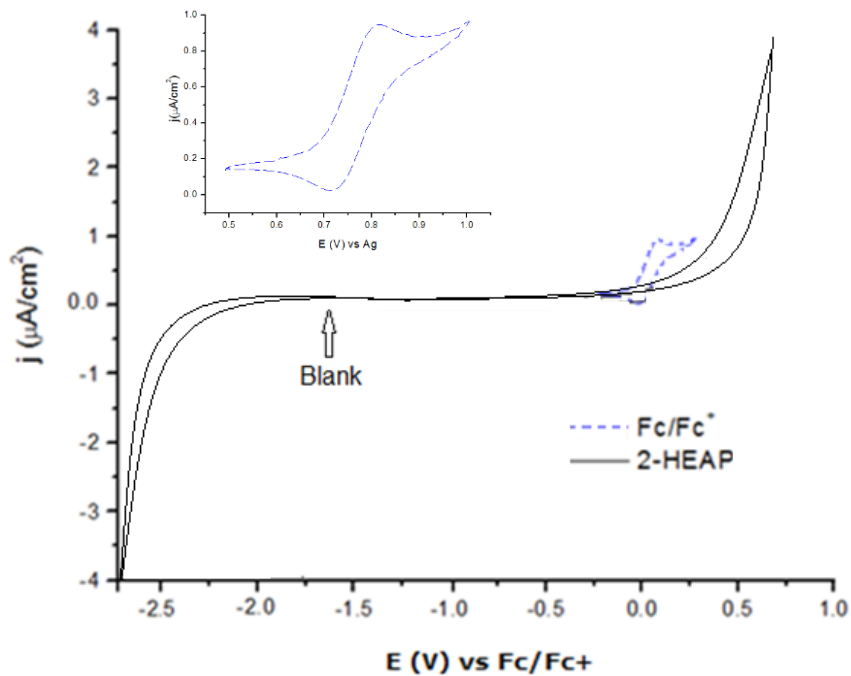


Figure 1. Cyclic voltammogram of the 2-HEAP IL (blank) with internal reference of ferrocene 5mM (small voltammogram). 5mV/s. Room temperature. WE: ITO; pRE: Ag; CE: Pt. Inset: internal reference of ferrocene 5mM. 5mV/s. Room temperature. WE: ITO; pRE: Ag; CE: Pt.

Also, we show the electrochemical response of ferrocene in the RTIL 2-HEAP. Ferrocene is used as an internal redox reference according to the redox system $\text{Fc} \rightarrow \text{Fc}^+ + \text{e}^-$, with a potential value of 0.71V, in reference to the silver pseudo-reference electrode (Fig. 1) [36].

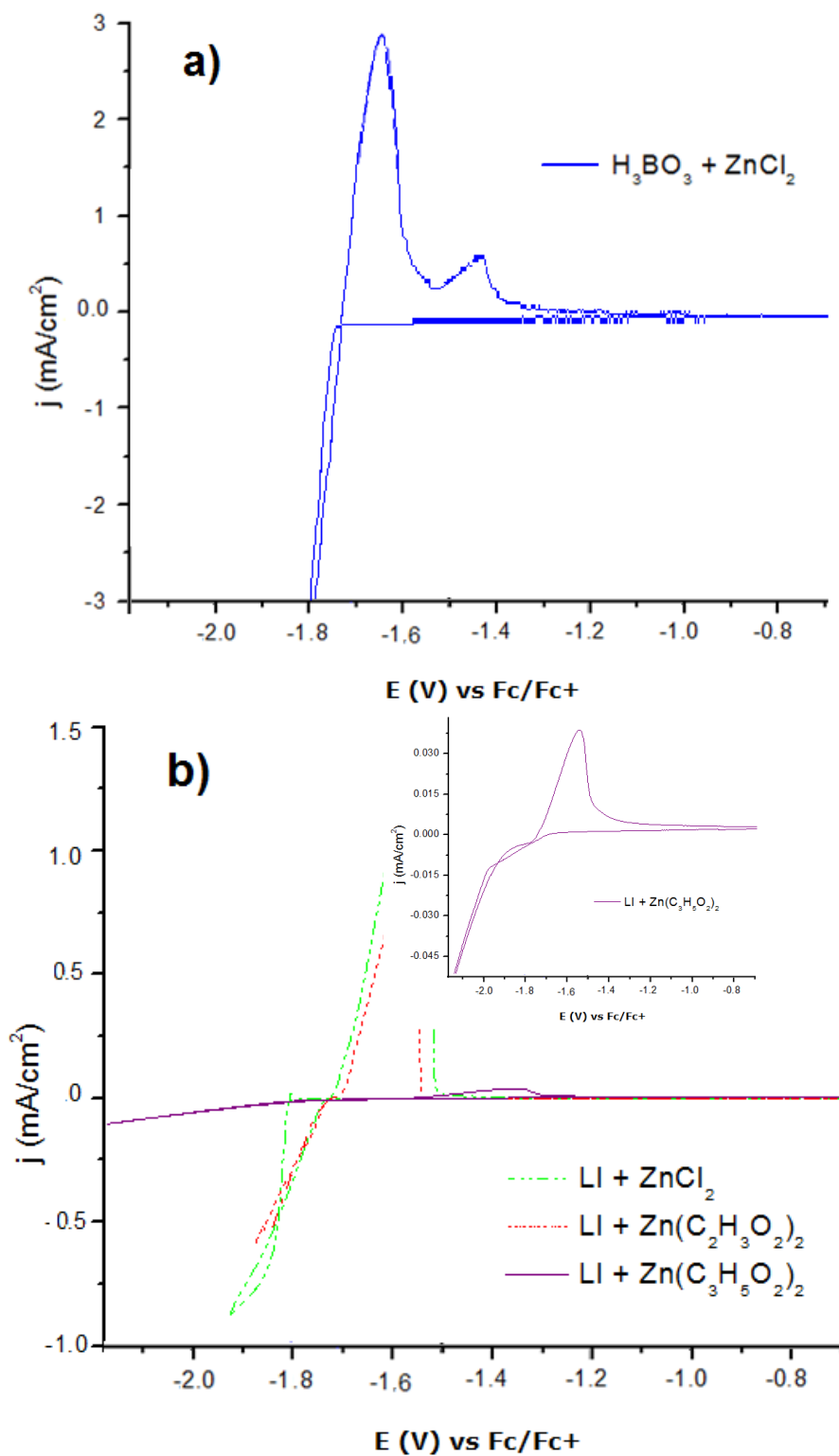


Figure 2. Cyclic voltammograms of **a)** 0.4M H_3BO_3 and 0.05 M ZnCl_2 in aqueous solution WE: ITO; RE: SCE; CE: Pt; and **b)** 2-HEAP IL with 0.05M ZnCl_2 , Zn acetate or Zn propionate in each case, WE: ITO; pRE: Ag; CE: Pt. 5mV/s. 25°C. Inset: 2-HEAP IL with Zn propionate, WE: ITO; pRE: Ag; CE: Pt. 5mV/s. 25°C.

It is common to use the ferrocene redox couple as an internal potential reference [37] in electrochemistry when organic solvents are used as electrolytes or common references electrodes (SCE, Ag/Ag⁺, etc.) could interfere or contaminate the system. It is necessary to say in this part that this study was carried to verify the stability of the pseudo-reference electrode in the IL, because its use in ionic liquids has been reported as a suitable reference system for potential measurements [35, 36]. This internal reference system allows to define a potential scale in 2-HEAP that can be compared with potentials measured in another media.

Fig. 2 shows the typical electrochemical response obtained by cyclic voltammetry from Zn(II) solutions in water and in 2-HEAP. These voltammograms were obtained at a scan rate of 5 mV/s and show to the electrochemical behavior of Zn(II) onto ITO in an aqueous solution (Fig. 2a) and in 2-HEAP (Fig. 2b); in this last case, salts used were ZnCl₂ (green, dash dot dot line), zinc acetate (red, dot line) and zinc propionate (purple, solid line). In order to represent all voltammograms in the same figure, the measured potential values either against SCE in aqueous medium or Ag pRE in 2-HEAP were referred to the Fc/Fc⁺ redox couple potential.

From figure 2b, a decrease in the cathodic limit of 2-HEAP is observed (near to -2.0V vs -2.5V) in the presence of Zn(II) salts, indicating that the reduction of Zn^(II) to Zn⁰ is carried out simultaneously with the electrochemical reduction of the solvent, as discussed later, which causes higher values of current to lower values of potential with the consequent decrease in the electrochemical window of 2-HEAP. It is necessary to note that this effect is smaller when zinc propionate is used as Zn(II) source. In general, in the studied conditions, in 2-HEAP, the global process involves the Zn(II) reduction but also the formation of molecular hydrogen as a direct product of the reduction of the cation of 2-HEAP. This effect is similar to that reported for nickel and silver electrodeposition in this ionic liquid [34].

In aqueous medium, a similar behavior is also observed but with a more notorious effect of the presence of zinc on the cathodic limit of the electrochemical window. In this case, higher currents associated to the simultaneous hydrogen evolution reaction were observed. In addition, as shown in Fig. 2a, contrariwise to the single oxidation process observed in 2-HEAP, in aqueous solution two oxidation peaks are observed. These peaks are associated to the oxidation of the hydrogen and of the metallic zinc, formed during the reduction scan. The simultaneous hydrogen evolution reaction as a secondary reaction during zinc electrodeposition has been widely studied and reported (1) and it is associated to the very high reduction potential required to carry out the reduction of zinc solutions and it is associated to the very high reduction power of metallic zinc [1].

In order to know the selectivity of the reduction process, assumed as directly related to the faradic efficiency, the electrical charges were calculated for both the anodic and the cathodic process from the integral of the electric current over time from the voltammograms of Fig. 2. The electrical charge was assumed to be associated only to faradic processes and the ratio between the anodic (Q_a) and the cathodic (Q_c) charges can be then indicates the faradic efficiency of the zinc reduction process and is assumed as the efficiency of the zinc electrodeposition. Then, higher value of the evaluated efficiency indicates a greater selectivity of the reduction processes. Results are shown in Table 1.

Table 1 shows the Zn salt influence in the efficiency of process: at the same inversion potential, a greater efficiency is obtained with Zn propionate in IL, as expected from Fig 2.

Table 1. Efficiency values obtained with the studied Zn(II) solutions.

$E_{inv} = -1.3V$	Qc	Qa	Efficiency
$H_3BO_3 + ZnCl_2$ (-1.2V)	-0.96995	0.361286	37.25%
IL + $ZnCl_2$	-3.8909E ⁻²	6.5418E ⁻³	16.81%
IL + Zn acetate	-0.101752	2.4712E ⁻²	24.29%
IL + Zn propionate	-8.606E ⁻²	8.592E ⁻²	99.84%

From Table 1, we observe also that working with the same salt but in a different electrolyte (IL or aqueous medium) a greater efficiency is obtained in the aqueous medium, but this efficiency is not only attributed to the Zn deposition, since also involves hydrogen evolution reaction. This result is that expected because of higher current densities in water, almost twice as much as in 2-HEAP, are observed at the same inversion potential for the aqueous solution. Anyway, expected from the voltammograms from Fig 2a for Zn propionate in 2-HEAP, the efficiency value indicates a null effect on the efficiency associated to the simultaneous occurrence of the HER.

Because of a good efficiency and then a good selectivity is observed when Zn propionate is used as zinc source, the dependence of the efficiency was studied as a function of the inversion potential for this salt in 2-HEAP. Table 2 shows that the inversion potential has an influence in the contribution of the reduction of the electrolyte on the cathodic charge and therefore, in the efficiency of process with Zn propionate in IL. A maximum is obtained at intermediate potentials and a similar evolution of the efficiency is observed for nickel electrodeposition in this medium [34]. This results allows to conclude that it is possible to carry out the selective electrodeposit of metallic zinc from zinc propionate solutions in 2-HEAP.

Table 2. Efficiency values as a function of the inversion potential for zinc propionate solutions in 2-HEAP.

IL + Zn propionate	Qc	Qa	Efficiency
$E_{inv} = -1.05V$	-3.425E ⁻⁵	9.986E ⁻⁷	2.92%
$E_{inv} = -1.1V$	-1.782E ⁻⁴	5.697E ⁻⁵	31.97%
$E_{inv} = -1.15V$	-1.205E ⁻³	5.765E ⁻⁴	47.84%
$E_{inv} = -1.2V$	-1.139E ⁻³	8.198E ⁻⁴	71.97%
$E_{inv} = -1.3V$	-8.606E ⁻²	8.592E ⁻²	99.84%
$E_{inv} = -1.5V$	-2.074E ⁻³	1.393E ⁻³	67.16%

In account of this results and in order to study in more detail the electrodeposition process of zinc, the effect of the value of the inversion potential on the electrochemical response has been carried out by using zinc propionate solutions in 2-HEAP .

The typical electrochemical response obtained for this system is shown in Fig 3. In the cathodic scan, two crossovers are observed at potentials A and B (E_A and E_B). This behavior is typical for process involving the formation of a new phase on the electrode surface with nucleation: the nucleation

potential is observed at E_A and its presence is typical of the formation of a new phase involving a nucleation process. The second crossover potential observed at E_B is associated to the open circuit potential and as reported in the literature [18, 34, 38, 39] this potential can be assumed as the open circuit potential of the system (E_{OC}) and can be associated to the thermodynamic equilibrium potential for the redox couple Zn^{2+}/Zn^0 in 2-HEAP. In the potential range of D region, the simultaneous process of the hydrogen evolution and zinc electrodeposition are carried out according to results shown in table2. On the other hand, when potential scan is reversed, only an oxidation peak is observed, with a maximum in current density at E_C (around -0.4 V). The current density associated to this peak is attributed to the oxidation of Zn formed during the cathodic scan.

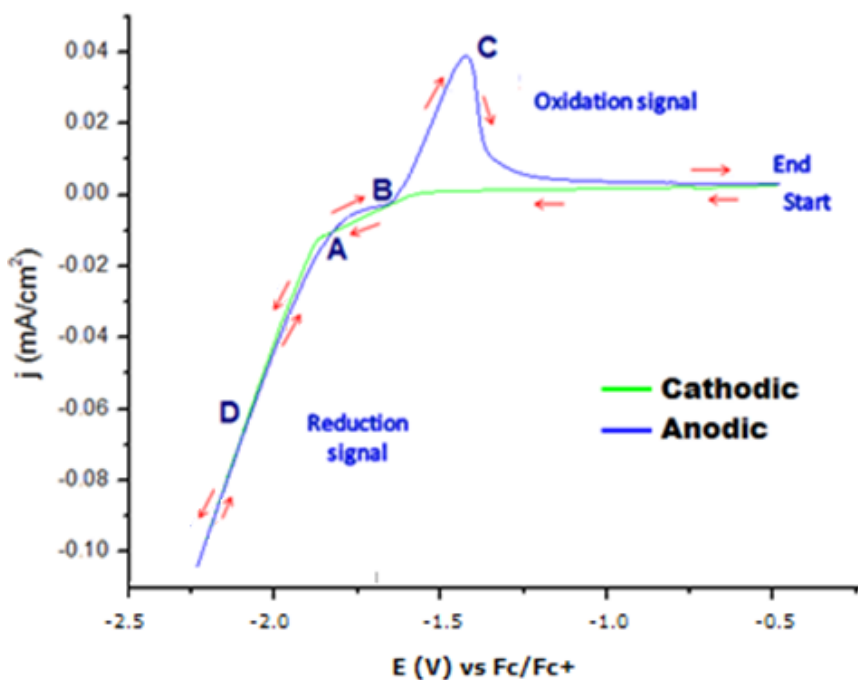


Figure 3. Cyclic voltammogram of 0.05M Zn propionate in 2-HEAP, WE:ITO; pRE: Ag; CE: Pt. 5mV/s. 25°C.

In order to identify the mechanism of the nucleation process for the Zn electrodeposition in 2-HEAP, a detailed study with chronoamperometric techniques was carried out. For that, two basic models, based either on an instantaneous or a progressive nucleation process, involving 1D, 2D or 3D growth and needles, disks cones or hemispheres particles, may be considered to fit the experimental results. Results are shown in Fig. 4. In our case, a simplified approach was defined to model the nucleation process. This approach involves a three-dimensional model with hemispherical nuclei and it is typical for electrodeposits obtained in these media [34, 35].

The models applied to fit the experimental results were developed by Scharifker [39-40] for instantaneous (1) and progressive (2) nucleation process with growth controlled by diffusion and 3D hemispherical nuclei. Models were applied to the normalized experimental curves and the follows equations associated to these models were applied:

Instantaneous nucleation:

$$\left(\frac{j}{j_m}\right)^2 = \frac{1.9542}{\left(\frac{t}{t_m}\right)} \{1 - \exp[-1.2564(t/t_m)]\}^2 \quad (1)$$

Progressive nucleation

$$\left(\frac{j}{j_m}\right)^2 = \frac{1.2254}{\left(\frac{t}{t_m}\right)} \left\{1 - \exp\left[-2.3367\left(\frac{t}{t_m}\right)^2\right]\right\}^2 \quad (2)$$

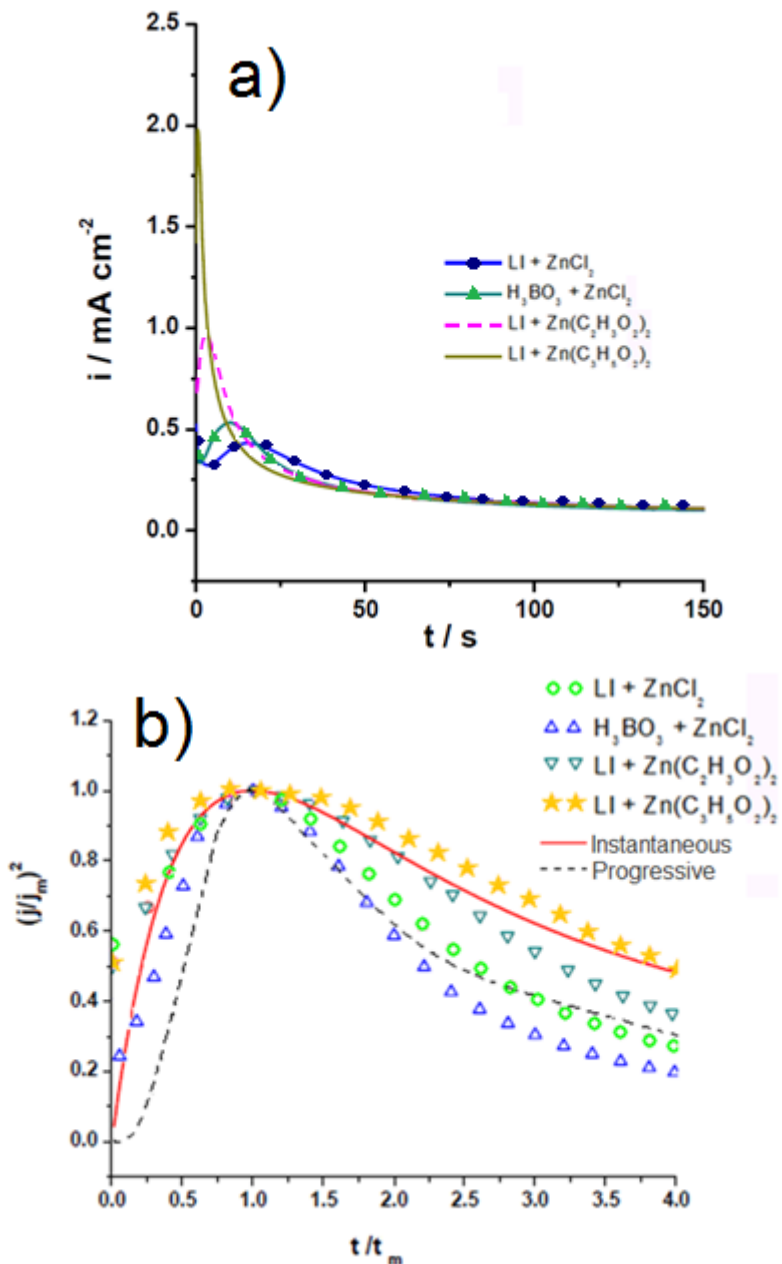


Figure 4. a) Current-time transients resulting from potential step experiments, and b) Normalized experimental transients of chronoamperometric response during Zn deposition in ITO, compared with both instantaneous and progressive nucleation models.

In these equations, j_m is the maximum current density in the current density transient and t_m is the time at this maximum point.

The main difference between the two nucleation models is related to the activation of the nuclei as a function of time: in the instantaneous nucleation model, a number fixed of nuclei are all activated at same time after a potential step and the crystal growth starts at same time that nucleation; contrariwise, in the progressive nucleation model, the nucleation sites (nuclei) gradually become activated and nucleus sites stars to growth as the chronoamperometric experiment is carried out [38,39].

In Fig 4a, the chronoamperometric response curves are in fact potentiostatic transients with a typical decay observed for all the studied salts. This decay is typical for metal electrodeposition process involving nucleation and growth steps [40]. According to the studied salt, three regions can be observed: a first region a very short times of capacitive current charge, with a very important decay in current followed of a second region where a raise in current is observed until to reach a maximum, after that current decreases according to the Cotrell equation [40]. This behavior is not only typical for nucleation process carried out in aqueous solutions but also in the electrodeposition from ionic liquids as reported by example by Wang [42] for zinc electrodeposition from hydrophobic ionic liquids. Differences observed in both the voltammograms and in the potentiostatic transients between solutions prepared with different salts are similar to these reported by Z. Liu [10, 42] and by Y. Song [43] when the influence of the anions in several ionic liquids and their mixtures have been studied. The observed effects have been associated to differences in the interactions at the surface level between the anions and the electrode or to solvation effects [44].

From Fig 4b, for the normalized experimental curves a better fit is observed for both ZnCl_2 aqueous and 2-HEAP solutions with the progressive nucleation model; contrariwise, for the zinc acetate and the zinc propionate solutions, the instantaneous nucleation model allow to obtain a better fit to the experimental results. These results were used to obtain the nucleation parameters, applying the corresponding nucleation model to fit the experimental results. The obtained nucleation parameters are shown in Table 3.

Table 3. Fitting parameters of Zn electrodeposition on ITO obtained with the Sharifker's electrocrystallization models.

	Aqueous medium	IL		
	ZnCl_2	ZnCl_2	Zn acetate	Zn propionate
E (V)	-1.05	-1.15	-1.2	-1.2
t_m (s)	15.37	9.93	2.91	0.38
J_m (Acm^{-2})	5.3×10^{-4}	4.3×10^{-4}	9.6×10^{-4}	1.97×10^{-3}
$J_m^2 t_m$ ($\text{A}^2 \text{scm}^{-4}$)	2.8×10^{-6}	2.8×10^{-6}	2.7×10^{-6}	1.5×10^{-6}
D ($\text{cm}^2 \text{s}^{-1}$)	7.4×10^{-6}	7.5×10^{-7}	7.1×10^{-7}	3.9×10^{-7}
N	4.9×10^5	3.1×10^5	1.7×10^6	2.4×10^7

Concerning the diffusion coefficients evaluated from the potentiostatic transients and shown in Table 3, their values are similar to those obtained by J.S. Keist [45] for zinc electrodeposition from an imidazolium based ionic liquid electrolyte. It is important to note that these diffusion coefficients are

smaller than those measured in aqueous solutions and the differences are directly attributed to the typical higher viscosities of the ionic liquids [46, 47].

Table 3 shows also the difference in the number of nuclei generated on the surface of the electrode according to the zinc salt used: the higher number of nuclei is observed when using Zn propionate in 2-HEAP and the lower number using $ZnCl_2$ in 2-HEAP. This phenomenon implies a more selective process at the surface and therefore a more uniform deposit with zinc propionate solutions as we can be seen in Figs. 5 and 6.

It is necessary to note that to apply the Sharifker's nucleation models is assumed that nucleation and the crystal growth are carried out involving a 3D-controlled diffusion process with hemispherical grains. This assumption is supported with the obtained SEM (Fig. 5) and AFM (Fig. 6) images which also show the existence of hemispheres evenly distributed over the electrode surface.

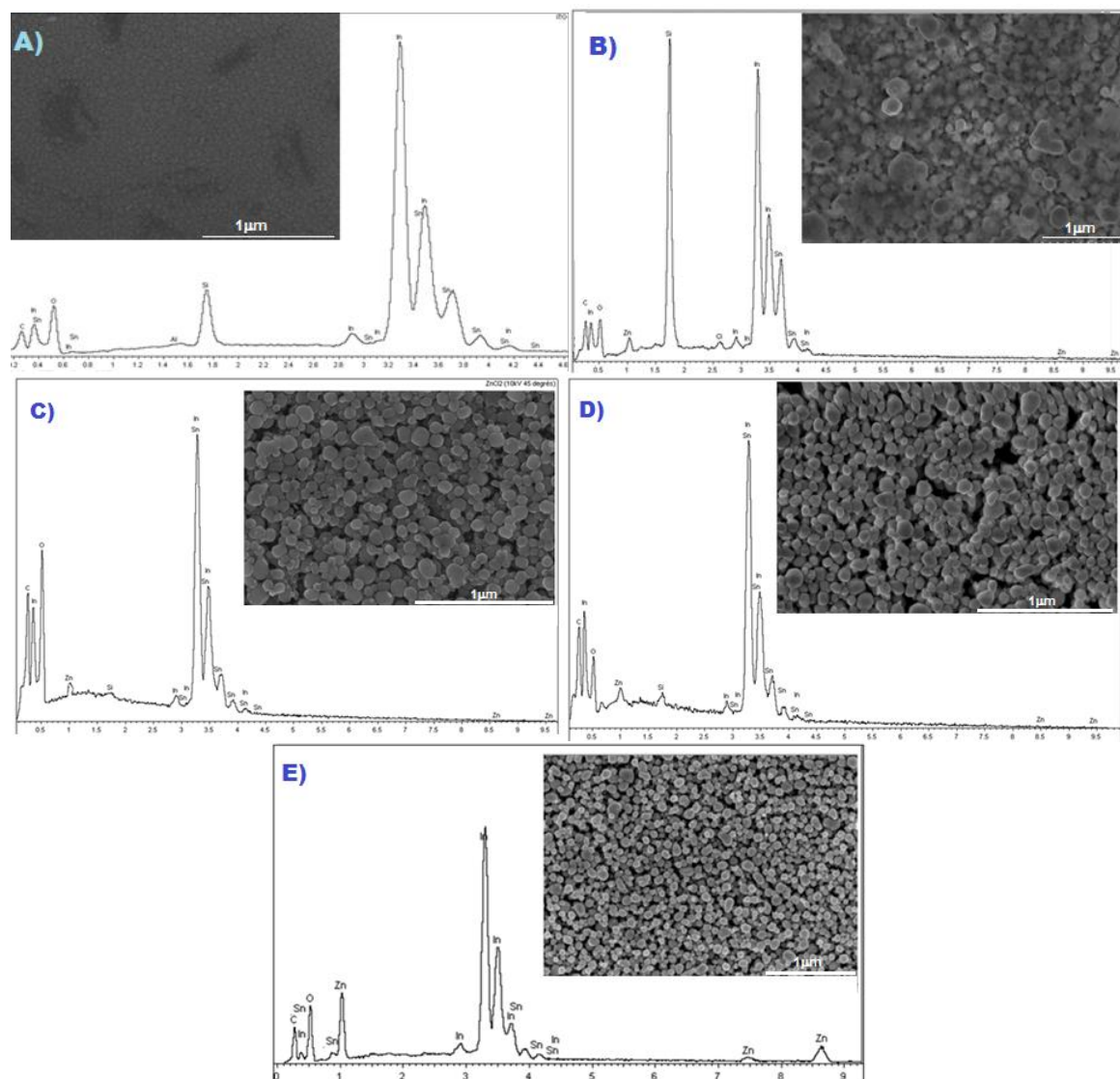


Figure 5. SEM and EDS images A) ITO, B) In aqueous experiment, C) IL with $ZnCl_2$, D) IL with Zn acetate, E) IL with Zn propionate.

Results of the study of the morphology of the electrodeposits by SEM and AFM show also that in all the studied solutions using 2-HEAP as solvent, compact and homogeneous zinc electrodeposits are obtained contrariwise to results obtained by Nieszporek [49] when zinc is electrodeposited from the aprotic ionic liquid 1-butyl 3-imidazolium chloride.

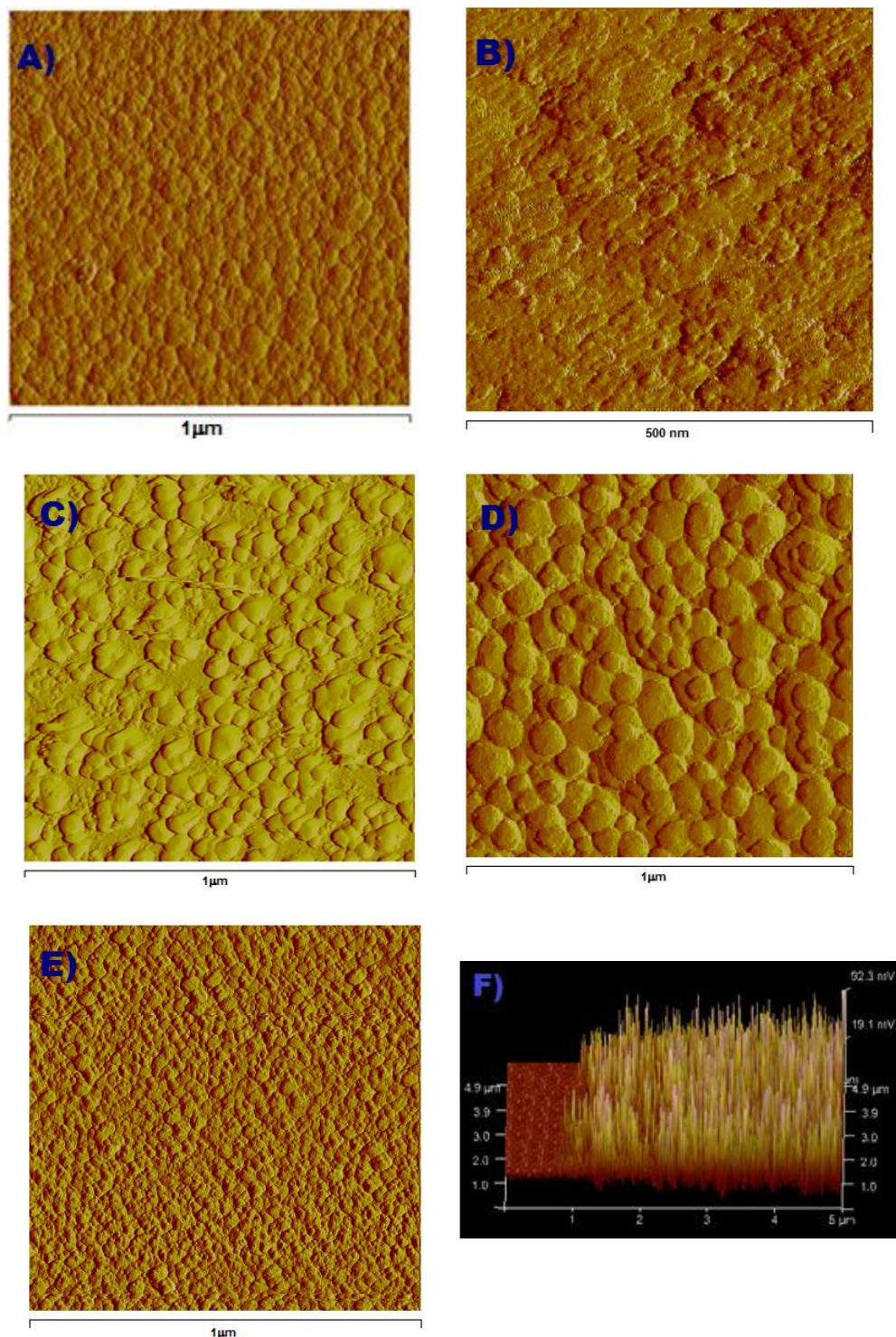


Figure 6. AFM images A) ITO, B) Zn from aqueous solution, C) Zn from ZnCl_2 in 2-HEAP D) Zn from Zn acetate in 2- HEAP, E) Zn from Zn propionate in 2-HEAP, F) as E) but cross section

The instantaneous nucleation process for Zn electrodeposited from zinc propionate solutions in 2-HEAP allows to explain the very smooth and homogeneous morphology of the deposits observed by SEM (Fig. 5) and AFM (Fig. 6). This effect of the nucleation mechanism on the morphology is quite different of the morphology of Zn electrodeposited from $ZnCl_2$ solution in 2-HEAP or in aqueous solution where deposits are formed following a progressive nucleation mechanism, less smooth deposits are obtained.

From images obtained using the AFM technique (Fig. 6) and applying the NanoScope Analysis 1.40 Software, it was possible to obtain the roughness values of the surface and the particle size (average, skewness and kurtosis) (Table 4); these results are corroborated with the profilometry technique used to measure a surface's profile, in order to quantify its thicknesses and get a 2D trace of topographic features on a surface. The thicknesses obtained were as follows: 100 nm in aqueous experiment, 200 nm in IL with $ZnCl_2$, 150 nm in IL with Zn acetate and 200 nm in IL with Zn propionate. Also all samples showed roughness to accord of the AFM results.

Table 4. Roughness coefficients, particle size and roughness profile evaluated by AFM

	ITO	Aqueous medium	IL		
	---	$ZnCl_2$	$ZnCl_2$	Zn acetate	Zn propionate
Roughness Rq (nm)	1.07	8.44	5.06	4.35	3.24
Roughness Sk (nm)	0.0696	-0.882	0.582	-0.351	0.097
Roughness Ks (nm)	1.52	3.35	2.88	2.31	2.20
Particle size (nm)	---	20-100	100-150	50-100	50-70

Results concerning roughness are in good agreement with the observed morphology from SEM and AFM images and allow to conclude zinc propionate solutions allow to obtain deposits with the lower roughness and then these solutions allow to obtain smooth and homogenous deposits.

Concerning the particle size, obtained results show that in the studied solutions is possible to obtain nanostructured deposits with grain sizes lower than 100nm contrariwise to zinc electrodeposits obtained from deep eutectic solvents which show an inhomogeneous morphology and grain sizes of $1.67 \mu m$ [49]. The lower grain sizes are obtained for the electrodeposits obtained from zinc propionate.

Elemental analysis by EDS (Fig. 5) and XRD (Fig. 7) showed the presence of Zn on the ITO confirming the formation of zinc electrodeposits. The presence of ZnO peaks are attributed to the zinc passivation, formed spontaneously when Zn layer is exposed to air. Peaks associated to the substrate (In and Sn signal) are always observed because of Zn is electrodeposited as a very thin film. The EDS analysis also show the presence of two unexpected elements, C and O, both of these elements were found only in the surface and most likely came from the exposure of the Zn deposits to the atmosphere. X-ray diffraction patterns of the deposited layers are shown in Fig. 7. Different phases are presents and these phases are assigned as Zn (101, 102) and ZnO (100, 101, 110). The intensities of the Zn peaks increase when the Zn deposition is carried out in IL 2-HEAP with Zn propionate.

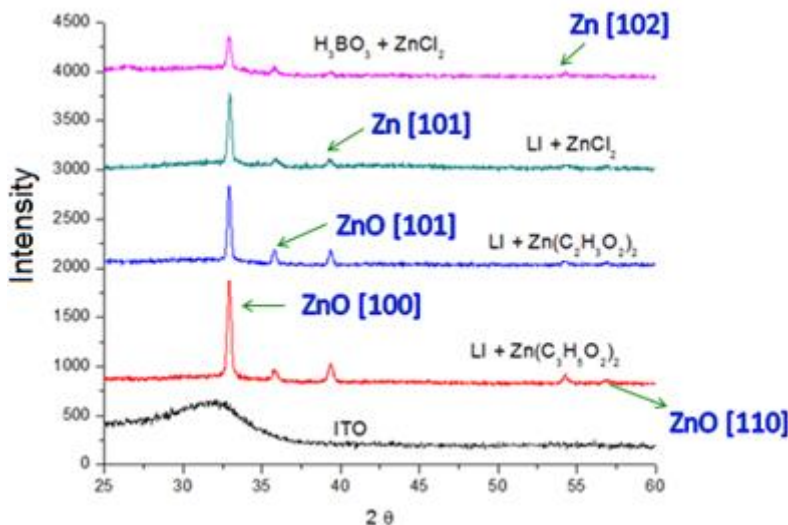


Figure 7. XRD data of electrodeposited Zn and ZnO on the ITO.

For the adhesion measurements, results are presented in Table 5. According to the applied technique, a good adhesion is related to a minimum of 20J/m². All deposits obtained from 2-HEAP show a good adhesion and a better adhesion than electrodeposits obtained from aqueous solutions.

Table 5. Comparison of zinc electrodeposited properties obtained.

	Aqueous medium	IL		
	ZnCl ₂	ZnCl ₂	Zn acetate	Zn propionate
Electrodeposits	Low adhesion Nonuniform	Good adhesion Uniform	Good adhesion Uniform	Good adhesion Uniform Reflective surface
Particle size (nm)	20-100	100-150	50-100	50-70
Roughness average (nm)	8.44	5.06	4.35	3.24
Thickness (nm)	100	200	150	200

4. CONCLUSIONS

Results obtained from the characterization and analysis of the obtained deposits allow to confirm that the electrodeposition of zinc depends both on the electrolyte nature (from 2-HEAP or aqueous medium) and the zinc salt used. Electrodeposits obtained from 2-HEAP are smoother and more homogeneous than from water and the best results are obtained when zinc propionate is used as zinc source. In this case, homogeneous electrodeposits of zinc are obtained, with a narrow distribution of grain size in the range of 50-70nm, contrarily to electrodeposits obtained from aqueous solutions with grain sizes from 20 to 100nm. In addition, the zinc electrodeposit obtained from aqueous media is produced simultaneously with HER, this limits the faradic efficiency of the electrochemical processes

and has also a direct effect on the nucleation and on the Zn electrocrystallization with some negative effects on the physical and structural properties of zinc electrodeposits obtained from these solution.

ACKNOWLEDGEMENTS

The authors are grateful to Thomas Dequivre and Elias Al Alam for measuring adhesion support. The financial support provided by CONACYT (México), project CB 2011 168032 and the Engineering Research Council of Canada (NSERC) are gratefully acknowledged.

References

1. R. Winand, *Modern Electroplating*, 5th ed. John Wiley & Sons, Inc., (2010) USA.
2. W. Lian-Kui, H. Ji-Ming, Z. Jian-Qing, *Corros. Sci.*, 59 (2012) 348.
3. T. J. Simons, A. A. J. Torreiro, P. C. Howlett, D. R. MacFarlane, M. Forsyth, *Electrochem. Comm.* 8 (2012)119.
4. A. Lasia, *Handbook of Fuel Cells, Fundamentals, Technology and Applications. Vol. 2.* , John Wiley & Sons, Inc., (2010) 416.
5. A. Döner, R. Solmaz, G. Kardaş, *Int J. Hydrot. Ener.* 36 (2011) 7391.
6. A. Kołodziejczak-Radzimska, T. Jesionowski, *Materials* 7 (2014) 2833.
7. M. Tulodziecki, J. M. Tarascon, P. L. Taberna, C. Guéry, *J. Electrochem. Soc.*, 159 (2012) D691.
8. S. Girish Kumar, K. S. R. Koteswara Rao, *RSC Adv.*, 5 (2015) 3306.
9. W. Zhong Lin, *J. Phys: Condens. Matter.*, 16 (2004) R829.
10. Z. Liu, S. Zein El Abedin, F. Endres, *Electrochim. Acta*, 89 (2013) 635.
11. B. Peric, J. Sierra, E. Martí, R. Cruañas, M. A. Garau, J. Arning, U. Bottin-Weber, S. Stolte. *J. Hazard. Mater.*, 261 (2013) 99.
12. D. J. Couling, R. J. Bernot, K. M. Docherty, J. K. Dixon, E. J. Maginn, *Green Chem.* 8 (2006) 82.
13. J. P. Hallett, T. Welton, *Chem. Rev.*, 111 (2011) 3508.
14. J. H. Davis Jr., *Chem. Lett.*,33-9 (2004) 1072.
15. N. V. Plechkova, K. R. Seddon, *Chem. Soc. Rev.*, 37 (2008)123.
16. C. A. Angell, Y. Ansari, Z. Zhao, *Faraday Discuss.*, 154 (2012) 9.
17. V. Sadhana, *Int. J. Bas. Sci. App. Comp. (IJBSAC)*, 1 (2014) 1.
18. Y. S. Liu, G. Pan, *Ionic Liquids for the Future Electrochemical Applications in Ionic Liquids: Applications and Perspectives*. InTechOpen. (2011) USA.
19. F. Endres, S. Z. Abedin, *Phys. Chem. Chem. Phys.*, 8 (2006) 2101.
20. J. Zhang, A. M. Bond, *Analyst*, 130 (2005) 1132.
21. R. X. Li, *Green solvents synthesis and application of ionic liquids*. Chemical Industry Engineering Press (2004), China.
22. M. C. Bubalo, K. Radošević, I. R. Redovniković, J. Halambek, V. G. Srček, *Ecotox. Environ. Safe.*, 99 (2014) 1.
23. M. Mahrova, F. Pagano, V. Pejakovic, A. Valea, M. Kalin, A Igartua, E. Tojo, *Tribol. Int.*, 82 (2015) 245.
24. M. Armand, F. Endres, D. R. MacFarlane, H. Ohno, B. Scrosati, *Nat. Mat.*, 8 (2009) 621.
25. M. V. Fedorov, A. A. Kornyshev, *Chem. Rev.* 114 (2014) 2978.
26. A. P. Abbott, G. Frisch, K. S. Ryder, (2013) *Annu. Rev. Mat. Res.*, 43 (2013) 335.
27. S. Eugénio, C. M. Rangel, R. Vilar, A. M. Botelho do Rego, *Thin Solid Films*, 519-6 (2011) 1845.
28. X. He, Q. Zhu, B. Hou, C. Li, Y. Jiang, C. Zhang, L. Wu, *Surf. Coat. Technol.*, 262 (2015) 148.
29. T. Jiang, M. J. Chollier Brym, G. Dubé, A. Lasia, G. M. Brisard, *Surf. Coat. Technol.*, 201 (2007) 6309.
30. A. Bakkar, V. Neubert, *Electrochem. Comm.*, 51 (2015) 113.

31. A. Pnkert, K. L. Ang, K. N. Marsh, S. Pang, *Phys. Chem. Chem. Phys.*, 13 (2011) 5136.
32. T. L. Greaves, C. J. Drummond, *Chem. Rev.* 108-1 (2007) 206.
33. S. Liao, H. J. Jhuo, P. Yeh, Y. Cheng, Y. Li, Y. Lee, S. Sharma, S. Chen, *Sci. Rep.*, 4 (2014) 6813.
34. S. López-León, R. Ortega-Borges, G. Brisard, *Int. J. Electrochem. Sci.*, 8 (2013) 1382
35. E. Cuara-Diaz, G. Brisard, G. Trejo, Y. Meas, R. Ortega-Borges, *Int. J. Electrochem. Sci.*, 7 (2012) 12856.
36. L. E. Barrose, A. M. Bond, R. G. Compton, A. M. O'Mahony, E. I. Rogers, D. S. Silvester, *Chem. Asian J.*, 5 (2010) 202.
37. D. Kozak, M. Panigrahi, M. Grabda, E. Shibata, T. Nakamura, *Electrochim. Acta*, 163 (2015) 41.
38. B. Scharifker, G. Hills, *Electrochim. Acta*, 28 (1983) 879.
39. E. Noam, E. Moshe *J. Biomed. Mater. Res. A.*, 80A (2007) 621.
40. O. Brylev, L. Roué, D. Bélanger, *J. Electroanal. Chem.*, 581 (2005) 22.
41. Y. Wang, H. Yeh, Y. Tang, C. Kao, P. Chen, *J. Electrochem. Soc.*, 164 (2017) D39.
42. Z. Liu, S. Z. El Abedin, F. Endres, *Chem. Phys. Chem.*, 16 (2015), 970.
43. Y. Song, J. Hu, J. Tiang, W. Gu, L. He, X. Ji, *ACS Appl. Mater. Interfaces*, 8 (2016) 3203.
44. Z. Liu, S. Z. El Abedin, N. Borisenko, F. Endres, *ChemElectroChem*, 2 (2015) 1159
45. J. S. Keist, *In-situ Analysis of Zinc Electrodeposition within an Ionic Liquid Electrolyte Ph. D. Dissertation*, University of California (2003) 31.
46. J. Z Yang, Y. Pin, W. Pan, *Acta Chim. Sinica*, 62 (2004) 2035.
47. Zh. Zhou, D. He, Z. Cui, G. Li, *J. Cent. South Univ.*, 15 (2008) 617.
48. D. Nieszporek, W. Simka, K. Matuszek, A. Chrobok, A. Maciej, *Solid State Phenom.*, 227 (2015) 143.
49. S. Ibrahim, A. Bakkar, E. Ahmed, A. Selim, *Electrochim. Acta*, 191 (2016) 724.

© 2017 The Authors. Published by ESG (www.electrochemsci.org). This article is an open access article distributed under the terms and conditions of the Creative Commons Attribution license (<http://creativecommons.org/licenses/by/4.0/>).